

Electronic structure of semiconducting  $\beta$ -NaSn

F. Springelkamp

*Solid State Physics Laboratory, Materials Science Center, University of Groningen, Melkweg 1, 9718 EP Groningen, The Netherlands*

R. A. de Groot

*Research Institute for Materials, Faculty of Science, University of Nijmegen, Toernooiveld, Nijmegen, The Netherlands*

W. Geertsma\* and W. van der Lugt

*Solid State Physics Laboratory, Materials Science Center, University of Groningen, Melkweg 1, 9718 EP Groningen, The Netherlands*

F. M. Mueller

*Research Institute for Materials, Faculty of Science, University of Nijmegen, Toernooiveld, Nijmegen, The Netherlands*

(Received 9 January 1985)

In this paper we report calculations on the electronic structure of solid NaSn. The NaSn crystal consists of almost perfect tin tetrahedra separated by sodium atoms. This peculiar crystal structure is reflected in the electronic structure. The density of states is determined predominantly by the tin tetrahedra, which are isoelectronic to the phosphorous molecule  $P_4$ . The Fermi level is positioned in a gap of the predominantly tin  $p$  states—the fully occupied  $p$  states correspond to bonding states of the tetrahedron and the empty  $p$  states just above the Fermi level correspond to antibonding  $p$  states. The role of the sodium atoms is to supply electrons for filling the bonding states and to keep the tin tetrahedra separated, thus prohibiting the formation of a metallic tin band.

## I. INTRODUCTION

The intermetallic compounds of the alkali metals with group-IVB elements (Si, Ge, Sn, Pb) form an interesting class of materials, exhibiting quite peculiar crystal structures associated with a variety of chemical-bond types.<sup>1</sup> As a consequence of the large difference in electronegativity between the constituent elements, the alloys tend to have saltlike properties. Such ionic compounds form the subject of chemical studies that seek to explain their valences in terms of charge transfer. Generally the number of possible compositions and crystal structures is remarkably large and the compositions may deviate strongly from the one corresponding to an octet electron configuration. Within the more restricted group of equiatomic compounds  $AB$ ,  $A$  being one of the alkali metals Na, K, Rb, Cs (but not Li) and  $B$  the group-IVB element, the crystal structures exhibit a remarkable similarity. They all contain tetrahedra formed by the  $B$  atoms. The crystal structures of all the alkali-lead and alkali-tin alloys are isomorphous<sup>2</sup> and so are those of KSi, RbSi, CsSi, KGe, RbGe, and CsGe.<sup>3</sup> The crystal structures of NaGe and NaSi are closely related to each other and to those of the compounds mentioned above.<sup>4</sup>

According to the "Zintl" model as explained in Refs. 1 and 5 these alloys can be formally described by the formula  $(A^+)_4(B_4)^{4-}$ , the  $(B_4)^{4-}$  ion being isoelectronic to the tetrahedral molecules  $P_4$  and  $As_4$ .<sup>6</sup> This suggests that the bonding within a Sn tetrahedron is largely covalent. The bonding within a pnictide tetrahedron has been investigated theoretically and experimentally by Goodman.<sup>7</sup> The Zintl concept explains also the existence of similar tetrahedra of Si in  $BaSi_2$  and of Tl in  $Na_2Tl$ .

Our attention was drawn to these compounds by an investigation of liquid Na-Sn alloys. These alloys clearly show effects due to strong chemical bonding. Near the equiatomic composition the resistivity peaks to values exceeding those characteristic for purely metallic behavior,<sup>8</sup> while the Na Knight shift exhibits a dip as a function of composition.<sup>9</sup> These phenomena indicate a depletion of conduction electrons.

Similar electronic effects have been found in liquid Li-Ge,<sup>10</sup> and K-Pb.<sup>11</sup> The high resistivities ( $> 1000 \mu\Omega \text{ cm}$ ) suggest that the solid crystalline compounds could be semiconducting. The effects in the liquid alloy have been ascribed to the persistence of tetrahedra, similar to those in the solid. This supposition was corroborated by neutron-diffraction experiments.<sup>12</sup> The peak observed at the low- $q$  side of the main liquid-structure-factor peak has been interpreted in terms of ordering of negatively charged Sn ions or clusters and positively charged Na ions. The shoulder at the high-wave-vector side of the main peak reflects the short Sn-Sn distances characteristic of the tetrahedra. It is expected that in the liquid state not all of the tin atoms participate in the clusters. A general discussion of the relation between liquid-state and solid-state properties has been given in Ref. 13.

Electrical conductivity measurements on amorphous Na-Sn and Cs-Sn films have been reported by Avci and Flynn.<sup>14</sup> They find a conductivity gap near the equiatomic composition; as a function of composition this gap is significantly broader for Cs-Sn than for Na-Sn. X-ray photoemission spectroscopy measurements of CsSn, which is also semiconducting, have been carried out by Bates *et al.*<sup>15</sup>

The crystal structure of  $\beta$ -NaSn has been determined by

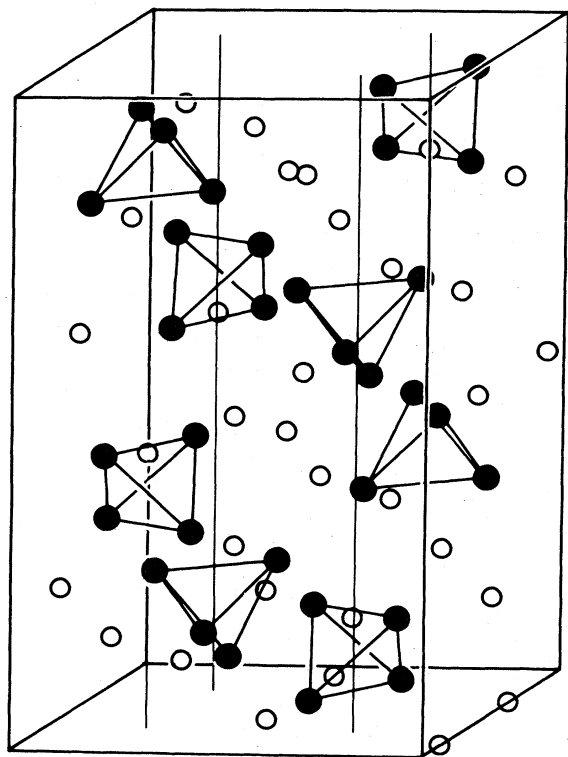


FIG. 1. The crystal structure of  $\beta$ -NaSn.

Müller and Volk.<sup>6</sup> It has a body-centered tetragonal unit cell with space group  $I4_1/acd$  ( $D_{4h}^{20}$ ) containing 64 atoms per unit cell (32 atoms per primitive unit cell). The Sn atoms occupy the 32  $g$  positions and the Na atoms both the 16  $e$  and the 16  $f$  positions. We clearly recognize the Sn tetrahedra (Fig. 1), separated by the Na atoms. Although the symmetry of the center of a tetrahedron in the crystal is only  $\bar{4}$  ( $S_4$ ) and not the full tetrahedral symmetry  $\bar{4}32m$  ( $T_d$ ) the interatomic Sn-Sn distances within the tetrahedra are equal within the experimental accuracy (0.2%) and amount to the 2.97 Å. In pure metallic Sn the four nearest neighbors are at 3.02 Å and the two next-nearest neighbors are at 3.17 Å. In the semiconducting gray Sn (which crystallizes in the diamond lattice) the four nearest neighbors are at 2.80 Å. Each tin atom in  $\beta$ -NaSn has only one next-nearest tin neighbor in a different cluster at a distance of 3.76 Å. Close examination of the structure reveals two independent three-dimensional networks of Sn tetrahedra. Although, at first glance, the structure looks rather complex, it can in fact be considered as an efficient way for densely packing tetrahedral clusters and Na spheres while keeping the tetrahedra as far apart as possible.

It is instructive to discuss first the electronic structure of the  $s$  and  $p$  levels of an isolated tetrahedral unit. The  $s$  states reduce to the  $\Gamma_1(A_1)$  and  $\Gamma_4(T_2)$  irreducible representations of the point group  $\bar{4}32m$  ( $T_d$ ), and the  $p$  states reduce to  $\Gamma_1(A_1)$ ,  $\Gamma_3(E)$ ,  $2^*\Gamma_4(T_2)$ , and  $\Gamma_5(T_1)$ . Calculations of the electronic structure of the isoelectronic,

tetrahedral  $P_4$  unit<sup>7</sup> show that the  $s$  levels  $A_1$  and  $T_2$  are far below the  $p$  levels. The  $p$  levels are split into three closely spaced low-lying (bonding) levels  $E$ ,  $T_2$ ,  $A_1$  and two high-lying (antibonding) levels  $T_1$  and  $T_2$ . The Fermi level is in the gap between the bonding levels and the antibonding levels. In the solid phase these levels broaden and form bands but it is possible that a gap still remains between the bonding and antibonding  $p$  levels. We expect a similar situation to occur for the Sn sublattice in  $\beta$ -NaSn.

Apparently, the formation of anion clusters is a basic property of the equiatomic alkali-group-IV compounds, in the liquid as well as in the solid. In previous papers<sup>13,16</sup> an approximate scheme for the band structure was proposed for these equiatomic compounds. The basic assumption is that the valence states are primarily determined by the deep anion potentials and thereby closely resemble the anion states. Essentially the band picture is then obtained by broadening the levels of the  $P_4$  configuration. The role of the Na atoms is restricted to donating electrons and keeping the tetrahedra apart, thereby obstructing Sn band formation.

It is the purpose of the present paper to give a more rigorous basis for this assumption by studying the band structure of crystalline NaSn in its real structure and a number of hypothetical structures in order to investigate the importance of the occurrence of tetrahedra and their embedding in the lattice. This paper is organized as follows. In Sec. II B 1 we describe the electronic structure of NaSn in the CsCl structure, i.e., without tetrahedra. In Sec. II B 2 a we describe the electronic structure of NaSn in a simple structure accommodating a Sn tetrahedron. Section II B 2 b deals with a more symmetric case with Sn tetrahedra. In Sec. II C we describe the electronic structure of the real  $\beta$ -NaSn lattice. In Sec. III we draw conclusions.

## II. THE ELECTRONIC STRUCTURE CALCULATIONS

### A. Details of the calculations

We used the augmented spherical wave method (ASW) developed by Williams, Kübler, and Gelatt, Jr.<sup>17</sup> to calculate the band structure. Scalar relativistic effects were included as described by Methfessel.<sup>18</sup> The inclusion of the spin-orbit interaction is described later. The potential is calculated self-consistently. The required input parameters are the positions and the atomic numbers of the constituent elements.

The most important approximations of the method are the use of a spherically symmetric potential within each Wigner-Seitz cell and the local-density approximation. In the calculations reported below we confined the core electrons of a certain atom to the corresponding Wigner-Seitz cell; i.e., effects due to direct kinetic transfer of core electrons between different cores are neglected. For real physical structures this approximation is justified.

Another question is the influence of the local-density approximation on the electronic structure of semiconductors. Usually this has the effect of making the band gap

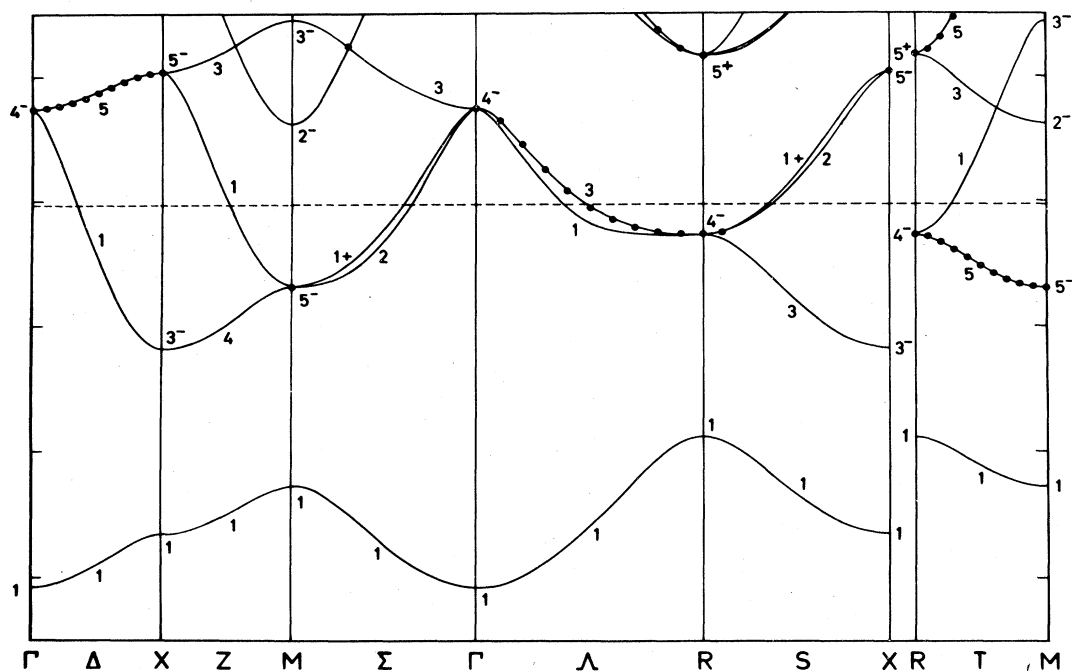


FIG. 2. The band structure of a fictitious NaSn alloy on a CsCl lattice.

about 30% too small. We have to keep this in mind when interpreting sizes of gaps obtained by this method.

#### B. The electronic structure of NaSn in some fictitious, simplified crystal structures

##### 1. The CsCl structure

One of the simplest equiatomic structures is the CsCl structure. We performed a band-structure calculation for Sn and Na situated at the lattice sites of this structure. The lattice parameter was 2.621 Å. We chose Wigner-Seitz radii of 2.137 Å and 1.6359 Å for Na and Sn, respectively. These radii were used throughout all the calculations reported here, unless specified otherwise. They result from an equilibration of the overlap between the various Wigner-Seitz spheres in the real  $\beta$ -NaSn crystal structure. The resulting band structure is shown in Fig. 2. There is one split-off Sn  $s$  band and a broad Sn  $p$ -band complex. The Fermi level intersects the  $p$ -band complex, which forms a continuous complex without a gap. The Sn  $d$  states are situated above the Fermi level.

##### 2. Electronic structure of fictitious NaSn alloys accommodating Sn tetrahedra

If, indeed, the band structure is largely determined by the Sn sublattice one may, by comparison with the electronic structure of  $P_4$ , expect a band gap as soon as Sn tetrahedra are introduced in the hypothetical structure. To test this hypothesis we designed some imaginary structures accommodating Sn tetrahedra.

*a. Structure with one tetrahedron per unit cell.* First a structure with one tetrahedron per unit cell in a tetragonal

crystal was considered. The density was taken to be equal to that of the real structure. The length of the  $c$  axis was chosen in such a way that the shortest distance between two Sn atoms in two different tetrahedra was in accordance with the real structure (Fig. 3). The dimensions of the tetragonal cell are  $a = 6.6000$  Å,  $c = 5.4603$  Å. The space group is  $P4(S_4^1)$ . The Sn positions are the 4  $h$  positions with  $x = 0.2242, y = 0, z = 0.1917$ . The Na positions are 1  $b$ , 1  $c$ , and 2  $g$  with  $z = 0.3083$ . Although in the resulting band structure the Sn  $s$  band is clearly split, there is still no band gap at the Fermi level in the Sn  $p$  density of states (DOS) (Fig. 4). Nevertheless one may say

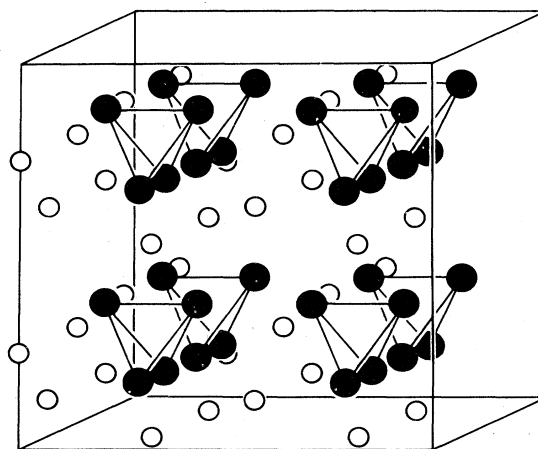


FIG. 3. A fictitious crystal structure for NaSn with one tetrahedron per unit cell.

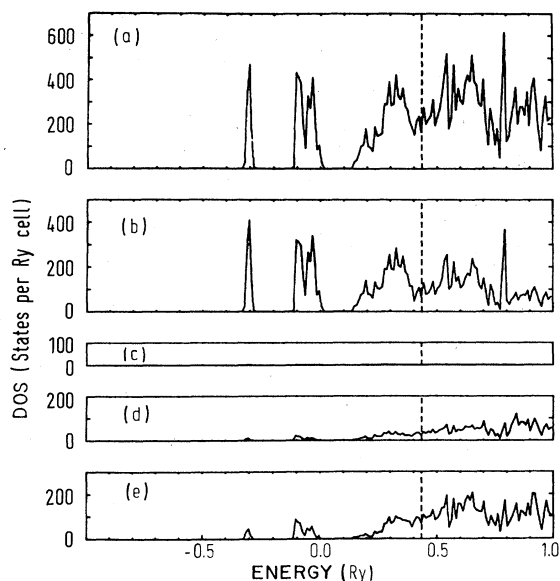


FIG. 4. The total and partial density of states of NaSn in the fictitious structure of Fig. 3.

that the Sn contribution to the DOS determines the shape of the valence-band structure. This follows clearly from a comparison of Figs. 4(a) and 4(b).

*b. Structure with Sn tetrahedra obtained by deformation of the NaCl structure.* In order to recognize the bands which cross the Fermi level we considered a structure with a space-group symmetry that accommodates the tetrahedron. Starting from the NaCl structure we contracted groups of 4 Sn atoms until they formed tetrahedra of the right size (Fig. 5). The density of the structure was

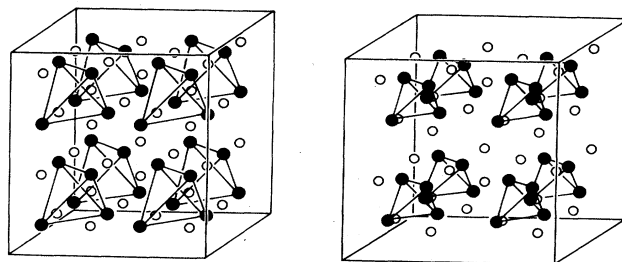


FIG. 5. By a contraction of groups of four Sn atoms in a NaCl structure (left) one can obtain a structure with tetrahedra and with the full tetrahedral symmetry (right).

equal to the experimental one. This leads to a cubic cell with space group  $P43m (T_d^2)$  and  $a = 6.1963 \text{ \AA}$ . The Sn atoms are at the 4  $e$  positions with  $x = 0.3305$  and the Na atoms are also at 4  $e$  with  $y = 0.75$ . In Fig. 6 we show the band structure along some illustrative high-symmetry lines in  $k$  space. If we compare the symmetries of the wave functions in the region of the  $p$  band with those of a single tetrahedron we find an extra band, intersecting the Sn  $p$  complex, which does not originate from the  $\text{Sn}_4$  tetrahedra. This band is of Na character, although hybridization with the Sn  $p$  complex occurs. The explanation of this effect is simple but instructive. In these artificial structures containing Sn tetrahedra the space left over by the Sn atoms consists of big cavities, whereas in the real structure each Na atom fits precisely in between the tin clusters. In the free-electron approximation strong direct Na-Na contacts lower the bottom of the Na band. Evidently mutual isolation of sodium atoms is a necessary

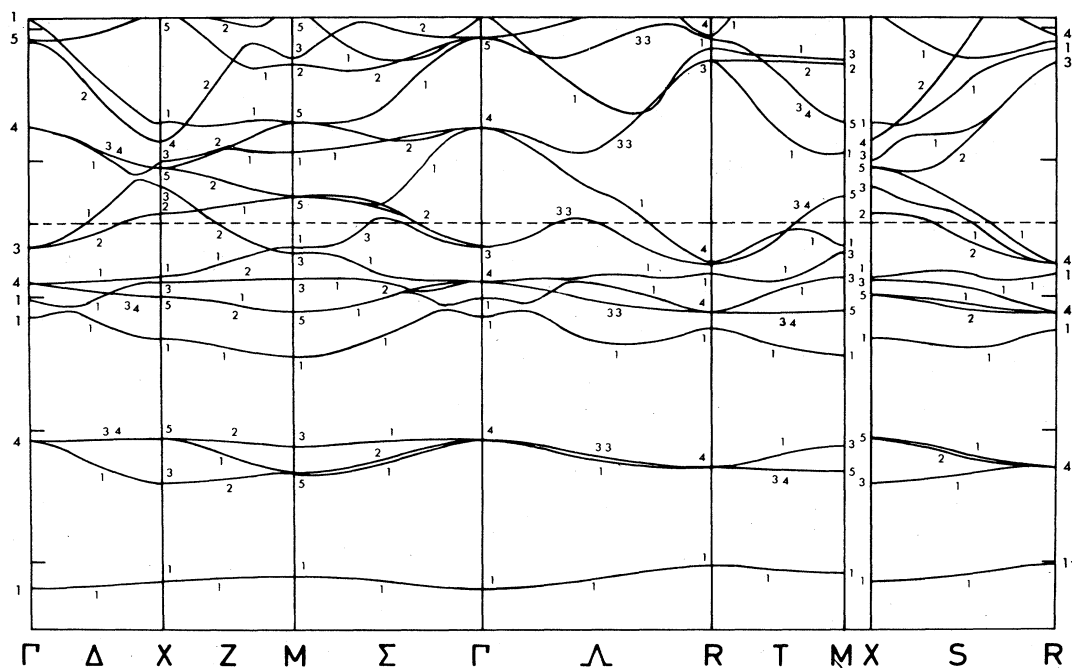


FIG. 6. The band structure corresponding to the highly symmetric case of Fig. 5. A sodium band passes through the Fermi energy.

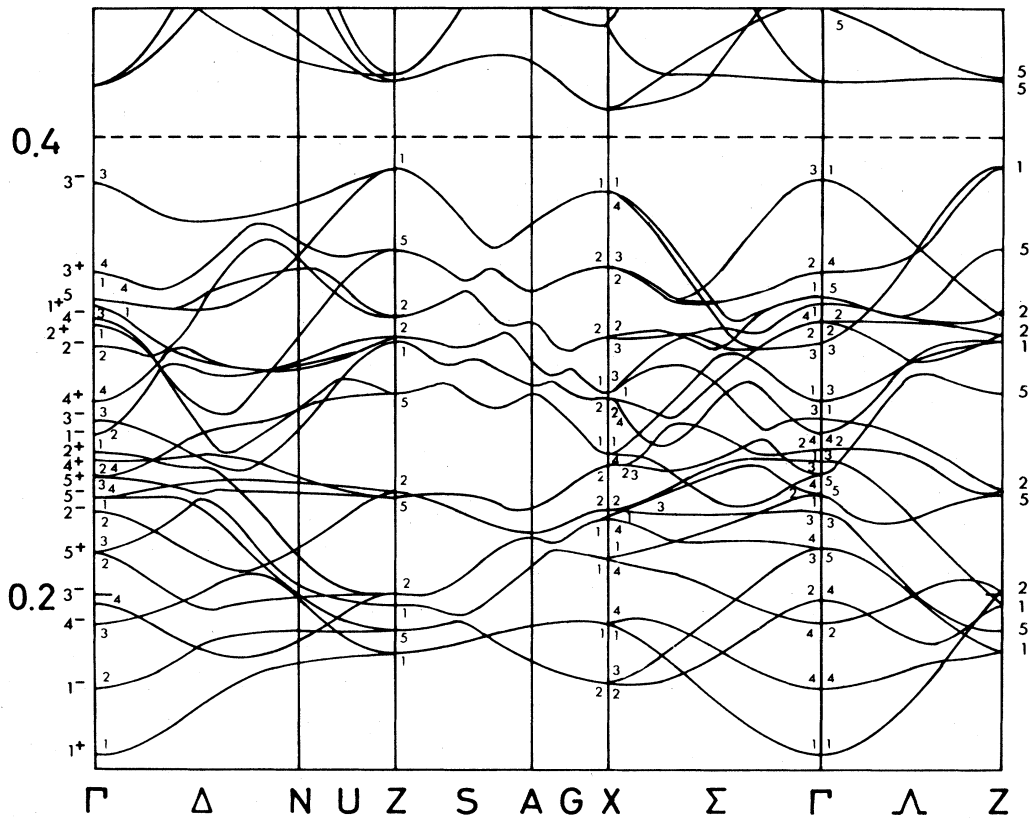


FIG. 7. The band structure of  $\beta$ -NaSn. Energies are given in rydbergs.

condition for the formation of a band gap in the Sn  $p$  density of states.

### C. The electronic structure of $\beta$ -NaSn

The band structure of the valence-band region is given in Fig. 7. The DOS for the valence band region is shown in Fig. 8. Also displayed are the decompositions of the wave functions inside the atomic Wigner-Seitz cells into the various angular momentum components of the wave functions (Figs. 9–11). We find that the Fermi level is situated in an indirect band gap between the top of the bonding bands at  $Z$  and the bottom of the antibonding bands at  $X$ . From the partial Sn DOS we note that this gap is situated in the center of the Sn  $p$  bands. The Sn  $s$  states form two separate narrow bands. The partial Na DOS in all angular momenta is rather similar to the shape of the total DOS. There is a general tendency for the low-energy side of any separate band to exhibit more Na  $s$  character than the high-energy side, while the middle- and high-energy regions exhibit more Na  $p$  or, respectively,  $d$  character.

The band structure shown in Fig. 7 has been calculated without spin-orbit coupling. Including this interaction at a few representative  $k$  points resulted in only minor changes ( $\sim 10$  meV). Evidently there is a strong quenching of orbital angular momentum. The results of the

band-structure calculations fit nicely into the following model.

As expected, the shape and energy positions of the valence band are primarily determined by the Sn tetrahedra. The scattering by the Na potential is weak, resulting

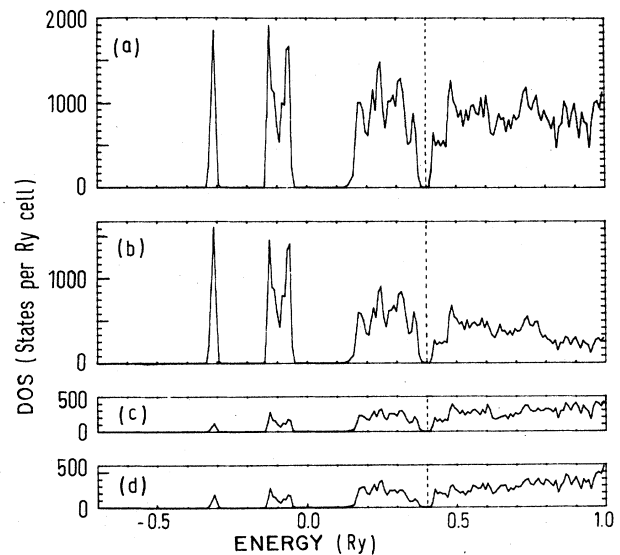


FIG. 8. The density of states of  $\beta$ -NaSn. (a) The total DOS and (b) the partial DOS of Sn, (c) partial DOS of Na in the  $16 e$  position, and (d) partial DOS of Na in the  $16 f$  position.

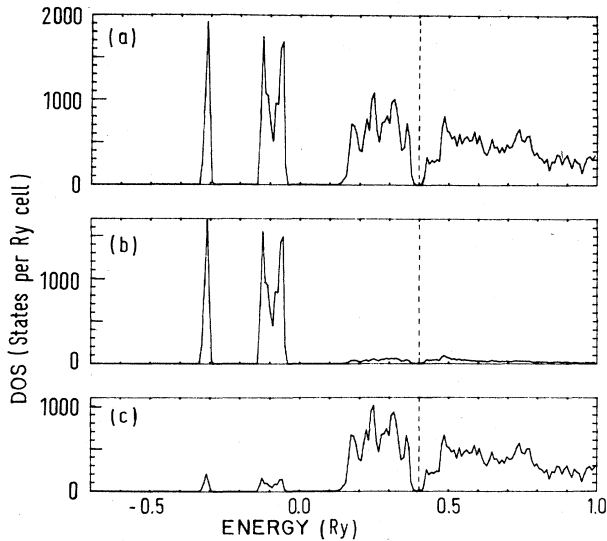


FIG. 9. The angular momentum decomposition of the partial DOS on Sn in  $\beta$ -NaSn. The  $s$  and  $p$  contributions are presented in (b) and (c) while the total Sn contribution is presented in (a). The  $d$  contribution is too small to be interesting.

in behavior of the Na Wigner-Seitz sphere similar to that of an empty position.

The Sn  $p$  bands form a band complex the shape of which follows directly from the tetrahedral Sn local environment: There is a splitting of the Sn  $p$  levels into two complexes, one with combinations of  $p$  orbitals which are *bonding within* the tetrahedra and one with combinations of orbitals which are *antibonding within* the tetrahedra. They are separated by an energy gap which contains the Fermi level. The bandwidth of both valence and conduction bands is determined by the interactions *between* the

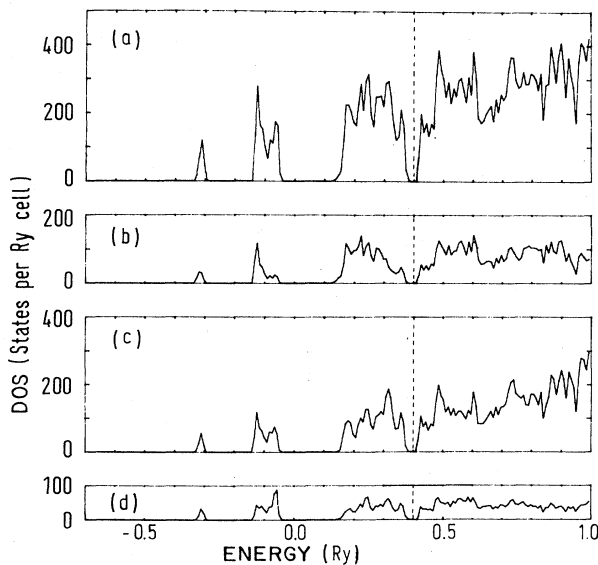


FIG. 10. The angular momentum decomposition of the partial DOS on Na at the 16  $e$  position in  $\beta$ -NaSn. The  $s$ ,  $p$ , and  $d$  contributions are presented in (b), (c), and (d), their sum in (a).

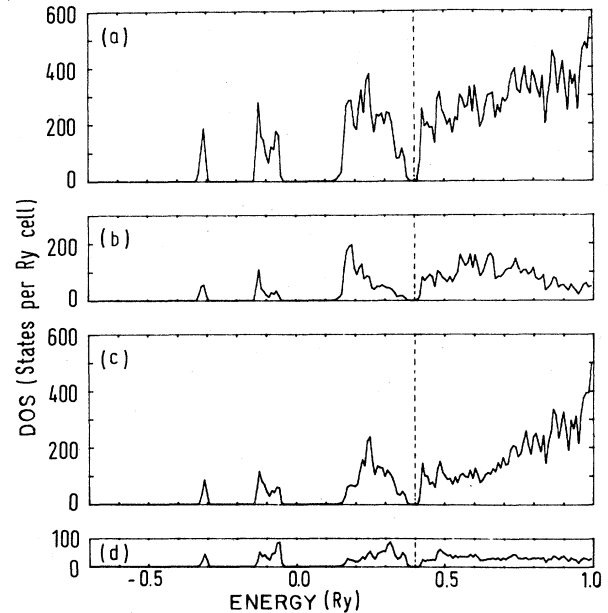


FIG. 11. The angular momentum decomposition of the partial DOS on Na at the 16  $f$  position in  $\beta$ -NaSn. The  $s$ ,  $p$ , and  $d$  contributions are presented in (b), (c), and (d), their sum in (a).

tetrahedra. Thus, one finds the following character for the Sn  $p$  states: the lowest-energy combinations are bonding *within* the tetrahedra as well as bonding *between* tetrahedra. With increasing energy the combinations remain bonding within tetrahedra but gradually become less bonding between tetrahedra until at the top of the valence band one finds combinations which are still completely bonding within the tetrahedra, but completely antibonding between the tetrahedra. Above the Fermi energy one finds  $p$  states of opposite character: the bottom of the conduction band consists of Sn  $p$  levels that are bonding between tetrahedra and antibonding within the tetrahedra. This character remains constant throughout the conduction band while the bonding character between tetrahedra gradually shifts as a function of energy until, at the top of the conduction band, the states are completely antibonding in all respects.

This model also explains the form of the partial density of states on the Na sites. The bottom of each band complex has bonding character between different tetrahedra. Consequently, the wave functions are even with respect to the bridging Na atoms and at their energies one finds Na  $s$  character only. At the middle and top of both valence and conduction bands this  $s$  character vanishes and is replaced by  $p$ -character (antibonding bridging over  $180^\circ$ ) and  $d$ -character (antibonding over  $90^\circ$ ) wave functions. This slight admixture of Na states stabilizes the  $p$ -band complex while at the same time it leads to a repulsion of the Na states to higher energies.

### III. CONCLUSIONS

The solid compound  $\beta$ -NaSn is a peculiar type of semiconductor. It is semiconducting in spite of the fact that

the constituent elements are metals and the electron count does not lead to a noble-gas electron configuration for the atoms (octet rule). The calculations confirm the intuitive picture that suggests similarity with white phosphorus ( $P_4$ ). Its semiconducting character is due to the fact that in the Sn clusters the  $p$  orbitals can form bonding states well separated from the antibonding states. The Fermi level is located in the gap between these two sets of states. It is not necessary to assume  $s$ - $p$  hybridization for this effect. The intrinsic position of the Na  $s$  states depends

critically on the environment of the Na atoms: the Na  $s$  states lie above the bonding Sn states only if the Na atoms are isolated from each other by the Sn clusters. The shape of the DOS is determined by the deepest potential involved, that of the tin atoms. The semiconducting properties of liquid NaSn can crudely be understood by the assumption of the persistence of local order in the liquid, as has also been found by using neutron diffraction. The interpretation of the Knight shift in the liquid systems, however, remains complicated.

- 
- <sup>1</sup>H. Schaefer, B. Eisenmann, and W. Muller, *Angew. Chem.* **85**, 742 (1973).  
<sup>2</sup>I. F. Hewaidy, E. Busmann, and W. Klemm, *Z. Anorg. Allg. Chem.* **328**, 283 (1964).  
<sup>3</sup>E. Busmann, *Z. Anorg. Allg. Chem.* **313**, 90 (1961).  
<sup>4</sup>J. Witte and H. G. Schnering, *Z. Anorg. Allg. Chem.* **322**, 260 (1964).  
<sup>5</sup>H. Schaefer and B. Eisenmann, *Rev. Inorg. Chem.* **3**, 29 (1981).  
<sup>6</sup>W. Mueller and K. Volk, *Z. Naturforsch.* **32b**, 709 (1977).  
<sup>7</sup>N. B. Goodman, L. Ley, and D. W. Bullett, *Phys. Rev. B* **27**, 7440 (1983).  
<sup>8</sup>C. van der Marel, A. B. van Oosten, W. Geertsma, and W. van der Lugt, *J. Phys. F* **12**, 2349 (1982).  
<sup>9</sup>C. van der Marel, P. C. Stein, and W. van der Lugt, *Phys. Lett.* **95A**, 451 (1983).  
<sup>10</sup>C. van der Marel, A. B. van Oosten, W. Geertsma, and W. van der Lugt, *J. Phys. F* **12**, L129 (1982).  
<sup>11</sup>B. P. Alblas, C. van der Marel, W. Geertsma, J. A. Meyer, A. B. van Oosten, J. Dijkstra, J. C. Stein, and W. van der Lugt, *J. Non-Cryst. Solids* **61& 62**, 201 (1984).  
<sup>12</sup>B. P. Alblas, W. van der Lugt, J. Dijkstra, W. Geertsma, and C. van Dijk, *J. Phys. F* **13**, 2465 (1983).  
<sup>13</sup>W. van der Lugt and W. Geertsma, *J. Non-Cryst. Solids* **61& 62**, 187 (1984).  
<sup>14</sup>R. Avci and C. P. Flynn, *Phys. Rev. B* **19**, 5967 (1979).  
<sup>15</sup>C. W. Bates, P. M. Th. M. van Attekum, G. K. Wertheim, K. W. West, and D. N. E. Buchanan, *Phys. Rev. B* **22**, 3968 (1980).  
<sup>16</sup>W. Geertsma, J. Dijkstra, and W. van der Lugt, *J. Phys. F* **14**, 1833 (1984).  
<sup>17</sup>A. R. Williams, J. Kuebler, and C. D. Gelatt, Jr., *Phys. Rev. B* **19**, 6094 (1979).  
<sup>18</sup>M. Methfessel and J. Kuebler, *J. Phys. F* **12**, 141 (1982).